INTERFACE

royalsocietypublishing.org/journal/rsif

Research

Cite this article: Metelmann S, Caminade C, Jones AE, Medlock JM, Baylis M, Morse AP. 2019 The UK's suitability for *Aedes albopictus* in current and future climates. *J. R. Soc. Interface* **16**: 20180761.
http://dx.doi.org/10.1098/rsif.2018.0761

Received: 29 October 2018
Accepted: 19 February 2019

Subject Category:
Life Sciences–Mathematics interface

Subject Areas:
biomathematics, biogeography, environmental science

Keywords:
Aedes albopictus, dynamic model, suitability analysis, diurnal temperature range, UK

Author for correspondence:
S. Metelmann
e-mail: soeren.metelmann@liverpool.ac.uk

Electronic supplementary material is available online at https://dx.doi.org/10.6084/m9.figshare.c.4418279.

THE ROYAL SOCIETY PUBLISHING

The UK's suitability for *Aedes albopictus* in current and future climates

S. Metelmann[1,3], C. Caminade[1,3], A. E. Jones[1], J. M. Medlock[3,4], M. Baylis[1,3] and A. P. Morse[2,3]

[1]Institute for Infection and Global Health, and [2]School of Environmental Sciences, University of Liverpool Liverpool, UK
[3]NIHR Health Protection Research Unit in Emerging and Zoonotic Infections, Liverpool, UK
[4]Medical Entomology Group, Public Health England, London UK

SM, 0000-0002-2394-5301; CC, 0000-0002-3846-7082; AEJ, 0000-0003-1273-5533; MB, 0000-0003-0335-187X; APM, 0000-0002-0413-2065

The Asian tiger mosquito *Aedes albopictus* is able to transmit various pathogens to humans and animals and it has already caused minor outbreaks of dengue and chikungunya in southern Europe. Alarmingly, it is spreading northwards and its eggs have been found in the UK in 2016 and 2017. Climate-driven models can help to analyse whether this originally subtropical species could become established in northern Europe. But so far, these models have not considered the impact of the diurnal temperature range (DTR) experienced by mosquitoes in the field. Here, we describe a dynamical model for the life cycle of *Ae. albopictus*, taking into account the DTR, rainfall, photoperiod and human population density. We develop a new metric for habitat suitability and drive our model with different climate data sets to analyse the UK's suitability for this species. For now, most of the UK seems to be rather unsuitable, except for some densely populated and high importation risk areas in southeast England. But this picture changes in the next 50 years: future scenarios suggest that *Ae. albopictus* could become established over almost all of England and Wales, indicating the need for continued mosquito surveillance.

1. Introduction

About 10 invasive species become established in Europe each year [1] and the UK alone spends about £1.7 billion annually to mitigate their impacts [2]. One of these species that has already invaded Europe and might now spread to the UK is the Asian tiger mosquito, *Ae. albopictus*. This mosquito spreads worldwide through its long-lasting and drought-resistant eggs that can be transported over long distances, for example, in used vehicle tyres or lucky bamboo pot plants [3]. The eggs can also undergo a diapause to resist colder winter temperatures [4], allowing temperate regions significantly colder than its original niche in South East Asia to be colonized. In Europe, *Ae. albopictus* was introduced in the late 1970s to Albania [5], in 1990 to Italy [6] and more recently into greenhouses in the Netherlands [7]. Since its introduction into Italy, it has rapidly spread along the Mediterranean coast and is now expanding its northern range [8].

This is a major concern as *Ae. albopictus* is an effective disease vector. It can transmit a range of arboviruses affecting humans and animals, including chikungunya, dengue and Zika viruses [9], as well as filarial worms [10]. In Europe, it was responsible for two outbreaks of chikungunya in Italy and a few cases of dengue in Croatia and France in the last 10 years [11–13]. In addition, it is a potent vector of zoonotic diseases because it feeds on mammals, birds, reptiles and amphibians [14], although it feeds preferentially on humans in urban areas [15]. So whether or not *Ae. albopictus* will spread from continental Europe to the UK and subsequently become established is of significant public

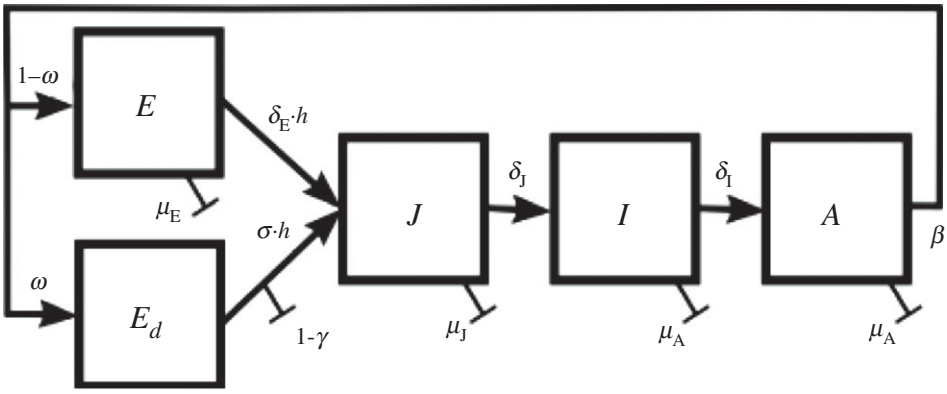

Figure 1. Life stages of *Ae. albopictus*. Eggs *E* hatch and become juveniles *J* (larvae and pupae). They develop to newly eclosed (immature) females *I* and finally to mature female adults *A*. Adult female mosquitoes lay normal eggs *E* in the summer months or diapausing eggs E_d at the end of the season. Diapausing eggs overwinter and are activated by a combination of longer day lengths, warmer temperatures and rainfall in spring.

health interest. And there is evidence for recent introductions: in September 2016, eggs were found in Kent, the English county closest to France, by a surveillance team of Public Health England [16], followed by another finding of eggs and larvae in July 2017 at another site in the same county [17]. Here, gravid females have probably been carried over in cars or lorries and subsequently laid eggs when released at motorway service points.

Mechanistic and statistical niche models have been developed to analyse the UK's climatic suitability for *Ae. albopictus*, suggesting that large parts of southern England are already suitable [18–20]. Dynamical models, better suited to capture the nonlinear behaviour of the mosquito's development, have been published more recently [21–24]. While all of these models use seasonal or daily mean temperatures and rainfall as drivers, it has become clear that the diurnal temperature range (DTR) significantly affects the life cycle of insects too. The DTR is the difference between the maximum midday temperature and the minimum night-time temperature. Studies on *Aedes* mosquitoes show that rates for development and mortality differ substantially under constant temperature conditions compared with a realistic diurnal temperature cycle [25–27]. Models that already incorporate DTR have been developed for aphids [28], moths [29], generic insects [30] and its effect have been recently applied to a model for *Anopheles* mosquitoes [31].

Here, we describe the development of a novel dynamical model for *Ae. albopictus* that explicitly incorporates the effect of DTR on its life cycle. We use mosquito occurrence data and container index (CI) data to evaluate the model performance before analysing the suitability of the UK for this invasive mosquito under current climate conditions and under two climate projection scenarios for the future.

2. Model and methods

Based on previous studies, we chose a compartmental, climate-driven approach to model the life cycle of *Ae. albopictus* [21,23,24]. The model comprises five differential equations. Details on climate-dependent variables can be found in electronic supplementary material, SI.1.

2.1. Dynamic life cycle model

The mosquito life cycle is described by five mosquito classes: normal, non-diapausing eggs *E*, juvenile aquatic stages *J*, immature female adults *I*, mature female adults *A* and diapausing eggs E_d (figure 1). Normal, non-diapausing eggs are laid during summer by mature females. Larvae hatch after eggs complete a development period and are activated by rainfall. The four larval stages and the pupal stage are combined into a single aquatic juvenile class in the model. Assuming a sex ratio of 50:50, juveniles then develop into newly eclosed male and female adults. Newly eclosed female mosquitoes do not directly show host-seeking behaviour. Instead, they first spend some time in a resting stage, only after which they take their first blood meal and start to lay eggs [32].

At the end of the season, the egg laying process depends on the photoperiod, *P*. When days are getting shorter, females start to lay diapausing eggs that do not hatch after a few days but overwinter. During the following spring, these eggs are ready to hatch when temperatures and photoperiod reach critical thresholds, and are eventually activated by rainfall.

All transitions from one class to another depend on temperature, *T*, and so do mortality rates. Because *Ae. albopictus*' water filled breeding sites are usually small [33], we use air temperature as a proxy for water temperature.

With parameter definitions given in table 1, model equations are as follows:

$$\frac{\mathrm{d}}{\mathrm{d}t}\mathbf{E}(t) = \beta(1-\omega)\mathbf{A}(t) - h\delta_{\mathrm{E}}\mathbf{E}(t) - \mu_{\mathrm{E}}\mathbf{E}(t),$$

$$\frac{\mathrm{d}}{\mathrm{d}t}\mathbf{J}(t) = h\delta_{\mathrm{E}}\mathbf{E}(t) + h\sigma\gamma\mathbf{E}_{\mathrm{d}}(t) - \delta_{\mathrm{J}}\mathbf{J}(t) - \mu_{\mathrm{J}}\mathbf{J}(t) - \frac{\mathbf{J}(t)^2}{K},$$

$$\frac{\mathrm{d}}{\mathrm{d}t}\mathbf{I}(t) = \frac{1}{2}\delta_{\mathrm{J}}\mathbf{J}(t) - \delta_{\mathrm{I}}\mathbf{I}(t) - \mu_{\mathrm{A}}\mathbf{I}(t),$$

$$\frac{\mathrm{d}}{\mathrm{d}t}\mathbf{A}(t) = \delta_{\mathrm{I}}\mathbf{I}(t) - \mu_{\mathrm{A}}\mathbf{A}(t)$$

and

$$\frac{\mathrm{d}}{\mathrm{d}t}\mathbf{E}_{\mathrm{d}}(t) = \beta\omega\mathbf{A}(t) - h\sigma\mathbf{E}_{\mathrm{d}}(t).$$

Development rates, δ, and mortality rates for eggs and juveniles, μ_{E} and μ_{J}, depend on the actual oscillating diurnal temperature *T*. The development from juvenile to immature females is halved in the equation for $(\mathrm{d}/\mathrm{d}t)I(t)$, $(1/2)\delta_J$, to account for the 50:50 sex ratio. Only the mortality rate for adults is derived from field data that already include a DTR. Daily mean temperatures, T_{mean}, are, therefore, used for μ_{A}. T_7 is the average temperature over the recent 7 days, used to trigger the spring hatching rate.

Table 1. Parameter definitions and values. Derivation and references of parameters are shown in electronic supplementary material, SI.1. Environmental drivers are temperature, T, rainfall, R, photoperiod, P, latitude, L and human population density, H. Please note that the environmental carrying capacity, K, and the egg activation by rainfall, h, are defined in equations (2.1) and (2.2) further down in the manuscript.

	parameter	value/formula
CTT_S	critical temperature over one week in spring (°C)	11.0☆
CPP_S	critical photoperiod in spring (hours)	11.25☆
$\sigma(T, P)$	spring hatching rate (1/day)	$\begin{cases} 0 & \text{if } T_7 < CTT_S \text{ or } P < CPP_S \\ r_S = 0.1^{\dagger} & \text{if } T_7 \geq CTT_S \text{ and } P \geq CPP_S \end{cases}$
$CPP_A(L)$	critical photoperiod in autumn (hours)	$10.058 + 0.08965\, L$
$\omega(P)$	fraction of eggs going into diapause	$\begin{cases} 0 & \text{if } P > CPP_A \text{ or } t < 183 \\ r_A = 0.5 & \text{if } P \leq CPP_A \text{ and } t \geq 183 \end{cases}$
δ_E	normal egg development rate (1/day)	1/7.1
$\delta_J(T)$	juvenile development rate (1/day)	$1/(83.85 - 4.89\, T + 0.08\, T^2)$
$\delta_I(T)$	first pre-blood meal rate (1/day)	$1/(50.1 - 3.574\, T + 0.069\, T^2)$
$\mu_E(T)$	egg mortality rate (1/day)	$-\ln(0.955 \exp(-0.5\,(\frac{T-18.8}{21.53})^6))$
$\mu_J(T)$	juvenile mortality rate (1/day)	$-\ln(0.977 \exp(-0.5(\frac{T-21.8}{16.6})^6))$
$\mu_A(T_{mean})$	adult mortality rate (1/day)	$-\ln(0.677 \exp(-0.5(\frac{T_{mean}-20.9}{13.2})^6)\, T_{mean}^{0.1})$
$\gamma(T_{DJF,min})$	survival probability of diapausing eggs (1/winter)	$0.93 \exp(-0.5(\frac{T_{DJF,min}-11.68}{15.67})^6)$
$\beta(T)$	egg laying rate (1/day)	$\begin{cases} 33.2 \exp\left(-0.5\left(\frac{T-70.3}{14.1}\right)^2\right)(38.8 - T)^{1.5} & \text{if } T \leq 38.8 \\ 0 & \text{if } T > 38.8 \end{cases}$
λ	capacity parameter (larvae · days /hectare)	10^6‡

☆[34].
†Best estimate.
‡[22,35].

Owing to the lack of information regarding the survival rates of eggs over long time periods (several months), we assume a survival probability γ of diapausing eggs that is dependent on the minimum winter temperature experienced, $T_{DJF,min}$. The survival probability is applied when eggs are activated in spring, see electronic supplementary material, SI.1 for details. Remaining diapausing eggs that have not hatched until August are removed.

Larval mortality not only depends on temperature but also on an environmental carrying capacity, K, representing juvenile competition and predation [36]. We use the model by White *et al.* [37] and its extension by Erguler *et al.* [24] to calculate K from rainfall, R, and human population density, H

$$K(R, H) = \lambda \frac{1 - \alpha_{evap}}{1 - \alpha_{evap}^t} \sum_{x=1}^{t} \alpha_{evap}^{(t-x)} (\alpha_{rain} R(x) + \alpha_{dens} H(x)). \quad (2.1)$$

As we model mosquito abundance in individuals per hectare, we keep the parameters at $\alpha_{evap} = 0.9$, $\alpha_{dens} = 0.001\ km^2$ and $\alpha_{rain} = 0.00001\ mm^{-1}$ [24] but multiply by a scaling factor λ to reach a maximum carrying capacity ranging between 500 000 and 800 000 individuals per hectare [22,35].

Similar to the carrying capacity, we model the hatching of eggs depending on rainfall and human population density. We use the rainfall-dependent approach by Abdelrazec & Gumel [38] and assume that up to $\epsilon_{rat} = 20\%$ of eggs can hatch in densely populated areas regardless of rainfall conditions:

$$h(R, H) = (1 - \epsilon_{rat}) \frac{(1 + \epsilon_0) \exp(-\epsilon_{var}(R(t) - \epsilon_{opt})^2)}{\exp(-\epsilon_{var}(R(t) - \epsilon_{opt})^2) + \epsilon_0} + \epsilon_{rat} \frac{\epsilon_{dens}}{\epsilon_{dens} + \exp(-\epsilon_{fac} H(t))}. \quad (2.2)$$

We set the optimal amount of daily rainfall to $\epsilon_{opt} = 8$ mm, and use $\epsilon_0 = 1.5$ and $\epsilon_{var} = 0.05\ mm^{-2}$ [38]. Density-dependent parameters are set to $\epsilon_{dens} = 0.01$ and $\epsilon_{fac} = 0.01\ km^2$, such that egg hatching is increased in areas where $H > 500$ people per km^2.

Note that other studies split the juvenile stage into larvae and pupae and some also split the mature female stage into host seeking, gestating, and ovipositing stages [22–24]. We also simulated these scenarios but they did not improve model fit to presence or CI data. As there was also more parameterization data available for a reduced model, we kept the model framework with a minimum number of equations. See electronic supplementary material, SI.2 for further details.

The model is implemented in *Octave v4.2.1* and Runge–Kutta 4 is used to solve ODEs. All scripts and a short example can be found in the electronic supplementary material.

2.1.1. Suitability index

We propose a suitability index E_0 that relates to the basic reproduction number R_0 in epidemiological studies. In

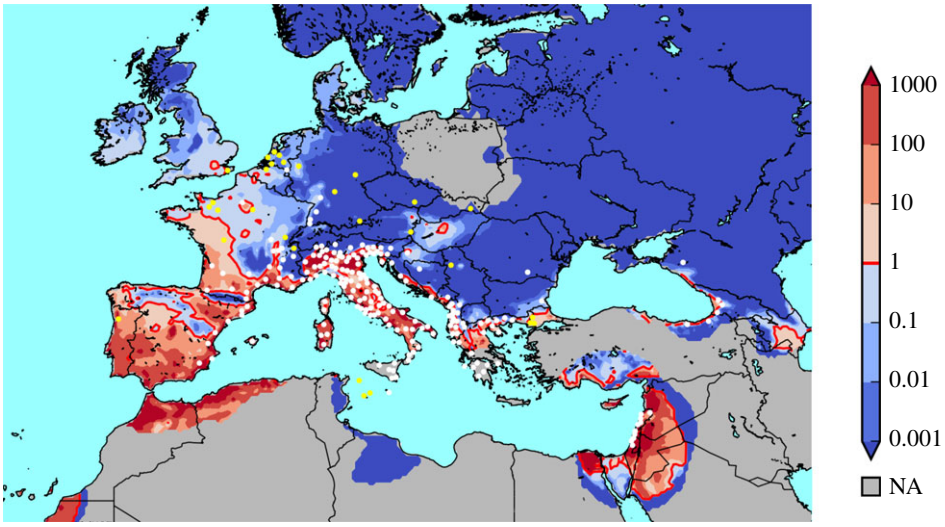

Figure 2. Spatial validation. White dots show established *Ae. albopictus* populations, yellow dots show one-time sightings. Background colours show the simulated suitability index of the period 2006–2016. Red contour distinguishes suitable ($E_0 > 1$) from unsuitable areas ($E_0 < 1$). In the grey area, climate data from the E-OBS dataset was incomplete for all years of the study period. (Online version in colour.)

epidemiology, R_0 is defined by the number of susceptibles infected by a single infectious individual in an otherwise uninfected population. Accordingly, we define our suitability index by the number of eggs that are produced at the end of a year, after placing a single (diapausing) egg at the beginning of the year into an uncolonized location. The amount by which the number of eggs has increased (suitable) or decreased (unsuitable) defines the suitability index E_i of that year i. Repeating this procedure for n consecutive years and taking the geometric mean of the yearly suitability indices gives the suitability index, E_0, for the according period,

$$E_0 = \sqrt[n]{\Pi_{i=1}^{n} E_i},$$

with $E_i = E_d(\text{day} = 365)/E_d(\text{day} = 1)$. Note that the crucial scaling of E_0 depends on the carrying capacity, K. With our standard settings, the model predicts about 1200 adult female *Ae. albopictus* per hectare for August/September in Rome (figure 7). This is well in the range of mark–release–recapture data, with an estimated 1400 females per hectare [39]. See electronic supplementary material, SI.3 for further details.

2.1.2. Diurnal temperature cycle

To calculate the DTR, we use the model by DeWit [40], which is well suited to compute realistic temperatures throughout the day from maximum and minimum temperatures [41]. Time points for temperature calculation are chosen according to the time steps for our explicit numerical solver, e.g. if $k = \frac{1}{100}$, we calculate 100 actual temperatures throughout the day at 0.14, 0.19, ... 24.00. Temperatures during day i are calculated by

$$T_i(h_t) = \begin{cases} \frac{T_{i-1}^{\max}+T_i^{\min}}{2} + \frac{T_{i-1}^{\max}-T_i^{\min}}{2}\cos\left(\frac{h_t+10}{10+t_s}\pi\right) & \text{if } h_t < t_s \\ \frac{T_i^{\max}+T_i^{\min}}{2} - \frac{T_i^{\max}-T_i^{\min}}{2}\cos\left(\frac{h_t-t_s}{14-t_s}\pi\right) & \text{if } t_s < h_t < 14 \\ \frac{T_i^{\max}+T_{i+1}^{\min}}{2} + \frac{T_i^{\max}-T_{i+1}^{\min}}{2}\cos\left(\frac{h_t-14}{10+t_s}\pi\right) & \text{else} \end{cases}$$

with $T_i^{\max/\min}$ being the maximum or minimum temperature of day i. The model assumes $T^{\min}$ at sunrise t_s and $T^{\max}$ at 14.00 local time. The time of day in hours is given by h_t, and the time of sunrise, t_s, is calculated using the daylight model by Forsythe *et al.* [42], depending on latitude, L, and the day of year, DOY. See electronic supplementary material, SI.4 for further details on the daylight model equations.

2.1.3. Climate and population density data

We run our model with a range of different climate data sets from historical records and future climate projections. For mosquito suitability in the UK, we compare the observed gridded climate datasets from E-OBS on a 25 × 25 km spatial scale [43] and from UKCP09 on a 5 × 5 km scale [44]. The E-OBS dataset is used for model validation over Europe and the ERG5 Eraclito dataset [45] is used for the model runs in the Emilia-Romagna region.

For future model runs across Europe, we use 25 × 25 km spatial scale climate projections from the NASA NEX-GDDP project [46] for two different emission scenarios, the medium RCP4.5 and the extreme RCP8.5 scenario. A subset of five general circulation models from the full set of 21 was chosen to represent the full range of uncertainty, see electronic supplementary material, SI.5 for details. For future changes, we focus on the period 2060–2069, the 2060s hereafter.

Human population density is based on the GPWv4 dataset [47]. For the 2060s projections, we assume the total UK population has increased from 65.5 million to 75 million [48] but has not changed in its spatial distribution.

2.2. Validation

2.2.1. Mosquito data

To validate the spatial distribution of suitability simulated by the model, we used *Ae. albopictus* occurrences [49], updated with data from the recent literature [16,17,50–53], and classified into established populations and one-time sightings according to the 2018 ECDC classification [8]. Occurrence points that were less than 25 km apart from one another were clustered together, resulting in a total of 234 out of 385 data points. We then checked whether each established occurrence point fell into a grid cell that was calculated to be suitable ($E_0 > 1$).

Figure 2 shows the suitability index for the period 2006–2016, which is highly consistent with occurrence data: 83% of the established populations fall into a suitable grid cell, 17% into unsuitable ones (excluding grid cells that are not covered

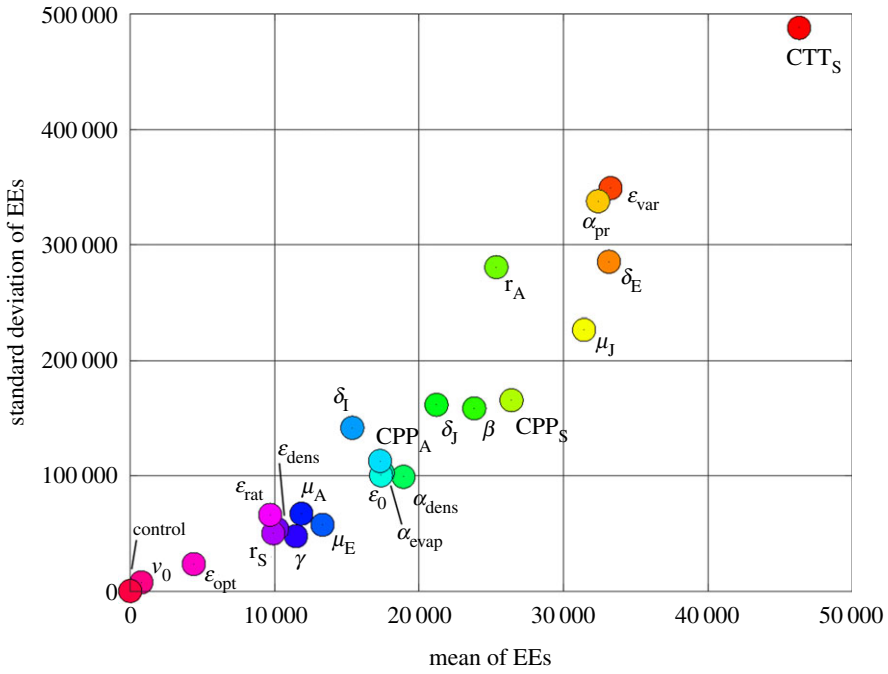

Figure 3. Elementary effects test. The higher the mean EEs, the more influential the parameter on the model outcome, E_0. The higher the standard deviation of the EEs, the larger its degree of interactions with other parameters. (Online version in colour.)

by climate data). However, the model misses some points in the southern Alps, the Bulgarian/Romanian Black Sea coast and some southern German cities. This is possibly because occurrences fall into warmer valleys or urban areas with microclimate conditions that are not captured by the coarse spatial resolution of the climate data. Also, the model predicts suitable conditions for areas such as southern Germany in most years but specific years with a very cold winter or dry summer lower the 10-year suitability index (compare electronic supplementary material, figure S7).

More densely populated areas, such as Madrid, Paris and London appear as suitable; they act as heat islands, further increasing mosquito development [54], and they supply mosquito breeding sites by man-made containers and irrigation.

We used observed CI data that are available for northern Italy to validate our model not only in space but in time (see electronic supplementary material, SI.7). While the onset and end of the mosquito season is well captured by the model, it sometimes over- or underestimates the peak in mosquito numbers at interannual timescale. The Pearson correlation between observed and simulated egg data is $r = 0.70$ (95% CI: $0.67 \leq r \leq 0.73$, $N = 996$).

2.2.2. Sensitivity analysis

To investigate the influence of each parameter on the final model output, E_0, we perform the elementary effects test (EET) [55]. The EET measures the influence of single input parameters on model outputs, as well as their degree of interaction with other parameters. Latin hypercube sampling is used to vary parameters in the range of $\pm 10\%$ of the standard setting [56]. The model is then run with the Italian climate data until convergence and the total egg number after 5 years is taken as reference. *Octave* scripts for these methods come from the SAFE toolbox [57].

The critical temperature threshold in spring, CTT$_S$, has the biggest effect on E_0, followed by parameters determining rainfall dependencies such as ϵ_{var} and α_{rain}, and egg development, δ_E (figure 3). Other mosquito-specific parameters range in the middle. Parameters such as initial egg numbers, v_0, or other hatching rate parameters, ϵ_{dens}, ϵ_{rat} and ϵ_{opt}, have a limited impact on the model output for the Italian climate settings. The distributions for mean and standard deviation of EEs indicate that parameters with a bigger effect on other parameters have a bigger effect on the model output, E_0.

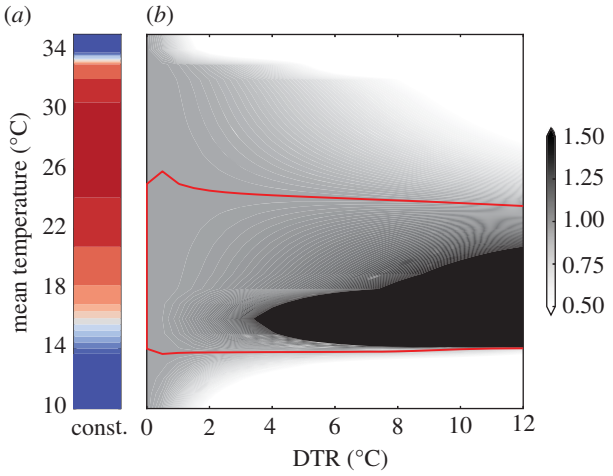

Figure 4. DTR impact on mosquito numbers. (*a*) Population size of *Ae. albopictus* measured in E_0 at constant temperature, with colour coding as in figure 2. (*b*) Relative population size after 365 days with diurnal temperature cycle compared to the population size experiencing constant temperatures (*a*). Values above 1 (within the red contour line) indicate where oscillating temperatures increase the population size. Mean temperature is given on the *y*-axis and the DTR is given on the *x*-axis. (Online version in colour.)

3. Results

3.1. Diurnal temperature range

To analyse the effect of the DTR on mosquito population size, we first run the model under constant conditions (5 mm

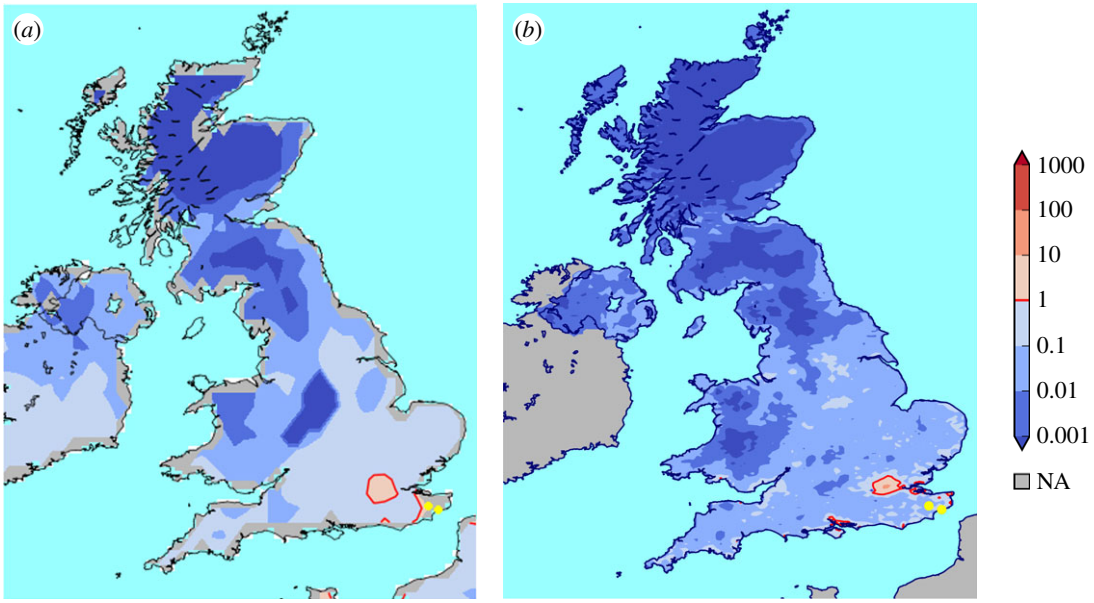

Figure 5. Suitability of the UK. Comparison of UK mosquito suitability at different spatial resolutions for the years 2006 until 2016, using E-OBS (*a*) and UKCP09 (*b*) climate data. Yellow dots show locations where *Ae. albopictus* has been found in 2016 and 2017. (Online version in colour.)

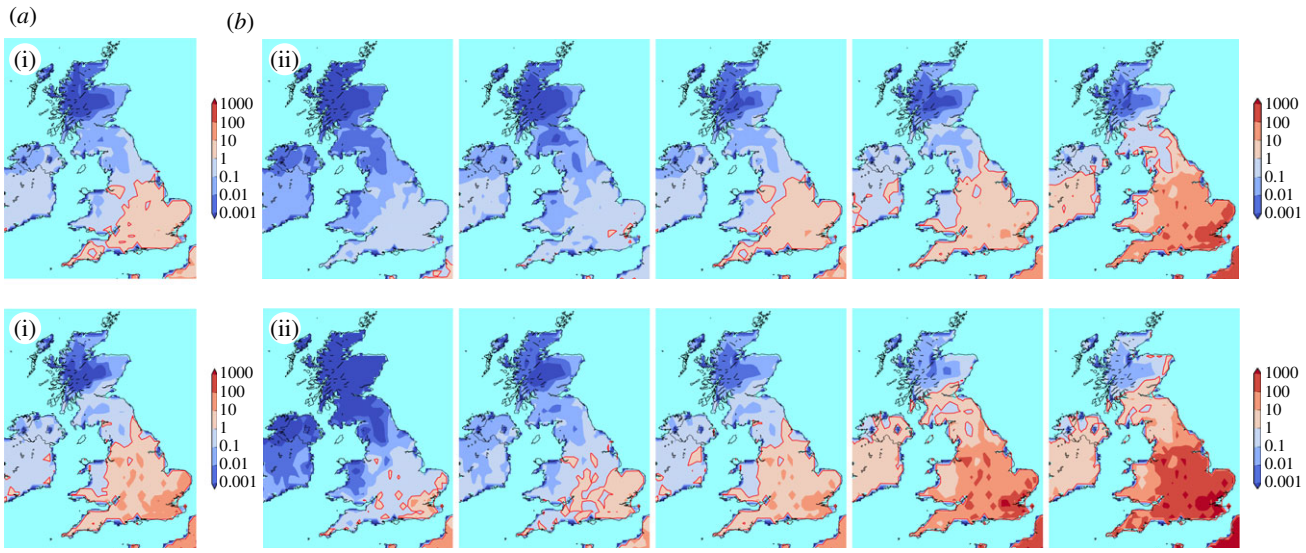

Figure 6. Future suitability of the UK. Suitability index for 2060–2069. (*a*) Geometric mean over all five model outputs for RCP4.5 (i) and RCP8.5 (ii). (*b*) Suitability index shown for each climate model individually for RCP4.5 (i) and RCP8.5 (ii). Left to right: minimum, 25th quantile, median, 75th quantile, maximum temperature increase for the British Isles. Climate models in order from the coldest to warmest are inmcm4, MRI-CGCM3, NorESM1-M, CanESM2, MIROC-ESM-CHEM for RCP4.5, and inmcm4, CESM1-BGC, NorESM1-M, CanESM2, MIROC-ESM-CHEM for RCP8.5. (Online version in colour.)

rainfall per day, 12 h daylight, 100 humans per km^2, starting with 1 egg per hectare) for a range of different temperatures. The model is run with constant mean temperatures (DTR = 0°C) and afterwards with oscillating temperatures (0°C < DTR ≤ 12°C), simulating the diurnal temperature cycle. We then compare absolute mosquito numbers after 365 days by dividing egg numbers that experienced DTR by egg numbers at constant temperatures.

Figure 4 shows that oscillating temperatures have a positive effect on the population size at lower mean temperatures, roughly for 14°C < T_{mean} < 24°C. This is actually the lower bound of the mosquito's suitable temperature niche, equilibria and stability analyses show that mosquito populations could survive at constant temperatures between approx. 13°C and 32°C (see electronic supplementary material, SI.9). Only when temperatures are very low (T < 13°C), DTR has a negative effect on the population numbers as mosquitoes experience high mortalities at the reached minimum temperatures. Electronic supplementary material, figure S12 shows more detailed time series of population growth at different temperature scenarios, these time series have been used to create figure 4. Including the DTR in simulations increases the suitability especially in northern regions compared with model runs that only use daily mean temperatures (electronic supplementary material, figure S11).

3.2. Current suitability of the UK

To analyse the UK's suitability for this mosquito, we run our model with two climate datasets for the recent period 2006–2016. Figure 5 shows that simulations driven by climate datasets with high and low spatial resolution agree in that the London

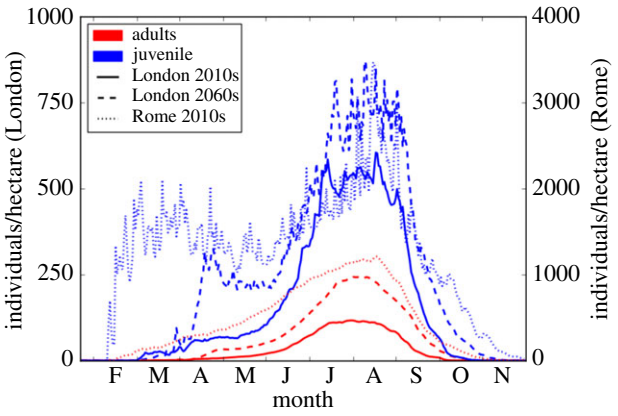

Figure 7. Mosquito season. Comparing the simulated length of the mosquito season in London in the 2010s and 2060s and with Rome in the 2010s. Means of 10 years for London and Rome 2010s data, based on E-OBS climate data. Future estimates are based on the ensemble mean of five RCP4.5 projection runs for 2060s. Note the different *y*-axis for London and Rome. (Online version in colour.)

area, the Thames estuary and parts of the southern coast are already suitable for the mosquito. Other warmer areas around the Severn estuary or in East Anglia, as well as populated northern regions such as Merseyside or around Sheffield are close to but not yet suitable. The Scottish Highlands, the Pennines and the Welsh mountains are unsuitable. Note that we are looking at a 10-year period to analyse the suitability for long-term establishment. We can also look at individual years, finding, for example, that 2016 was suitable over a larger region of the UK (see electronic supplementary material, figure S7).

3.3. Future suitability of the UK

Figure 6 shows the UK's future mosquito suitability for two emission scenarios, RCP4.5 and RCP8.5, for the 2060s.

Compared with recent UK suitability (figure 5), most of England will have become suitable for the establishment of *Ae. albopictus* populations in about 50 years when looking at the means. Parts of Wales might become suitable, depending on the emission scenario. Scotland and Northern Ireland remain mostly unaffected. However, there are large differences across the five climate models: only the southeast tip of the UK will become suitable with the coldest climate model, while almost the whole UK will become suitable with the warmest model.

Focusing on changes in seasonal abundance, simulations indicate that in current London, *Ae. albopictus* population sizes would be small in early summer and reach relative high number in July and August (figure 7). Future scenarios show an expansion of this peak into September and an overall increase in numbers. However, the length of the peak mosquito season would be short and population sizes remain low with respect to simulated values in Rome for recent climate conditions. Simulations for figure 7 were started 1 year ahead of the analysed period and mosquito numbers transferred from the end of a year into the next.

4. Discussion

Numerous studies investigating the climatic dependencies of *Ae. albopictus* have been published in recent years [4,58–63]. Taking these new findings into account and building on other modelling studies [21,23,24], we developed a dynamical model for *Ae. albopictus* that explicitly simulates the effects of rainfall for egg hatching and larval development, photoperiod for diapause induction and ending, and considers minimum and maximum temperatures that shape mortality and development rates of aquatic and adult stages.

The full temperature range experienced by mosquitoes in the field tend to increase model development rates throughout all stages. Mosquito populations at the lower temperature range (14°C to 24°C) develop better with oscillating temperatures. Here, night-time temperatures do not affect the development rates that are quite low anyway, while higher temperatures during the day significantly increase them [31]. Conversely, when mean temperatures are already high, lower night-time temperatures decrease development rates, while even higher temperatures during the day tend to increase mortality rather than development rates [27]. Thus, the DTR can be crucial for suitability analyses and should be considered for modelling the life cycle of mosquitoes and other insects [30,31], as it has already been done for the modelling of temperature-dependent viruses or malaria protozoans that mosquitoes can transmit [64–66].

Looking at the UK climate conditions for the past 10 years, we find large parts of the UK rather unsuitable for *Ae. albopictus*, except for some warmer and densely populated areas in the southeast of England. This finding suggests the mosquito has to be introduced into specific areas to enable long-term establishment. This result differs from findings by other modelling studies showing a medium to high suitability of larger parts of England [19,20,24,67] with up to five months adult mosquito activity in certain areas [18].

Our results are a bit more conservative because we included a rainfall-dependent mechanisms for egg hatching and larval mortalities in the model. Instead of constant egg hatching, we assumed that rainfall events lead to eggs being submerged under water and subsequent hatching. Similar to the finding of Tran *et al.* [22], the introduction of a rainfall-dependent egg hatching rate does not improve the model output fit to empirical abundance or ovitrap data. However, we found it enhances model performance in arid and unpopulated areas such as central Spain and Turkey.

We further assumed that a high human population density positively influences both the hatching of eggs and the survival of larvae because the mosquito is able to develop indoors [68], but also in arid but densely populated areas, where water storage and sprinkling create breeding habitats [69].

While large parts of England might not yet be suitable for a long-term establishment of this mosquito, individual years (especially the warmer recent ones, like 2016) already show a higher suitability which will continue to increase in the future [70]. Looking 50 years ahead, our projections suggest that *Ae. albopictus*, if introduced, could establish itself over most of England and southern Wales during the 2060s. The mosquito could become abundant in London during future summers; but even severe warming scenarios suggest that population sizes would still remain small with respect to current conditions in Rome, Italy. Large uncertainties related to the selected climate model and the emission scenario are due to the large variability of rainfall and temperature projections in the multi-model ensemble.

The question whether *Ae. albopictus* is able to spread from continental Europe to England is of great importance for public health and veterinary services. This mosquito is a

vector that can transmit pathogens that are present or constantly introduced into the UK, such as several arboviruses like Zika, dengue and chikungunya [71] and the canine heartworm *Dirofilaria immitis* [72]. Moreover, it is a very competitive species that could replace endemic mosquito species and become a biting nuisance to the local population [73]. Finding parts of southeast England already suitable and predicting a strong increase in suitability for most of England in the future, we highly recommend stringent vector surveillance in southern UK ports and high importation risk areas along motorways [3,74]. In addition, human and veterinary health services should get prepared to deal with pathogens transmitted by *Ae. albopictus* in warm summers [75], as it is recently happening in southern European countries.

Data accessibility. The E-OBS climate dataset for Europe is publicly available, following registration, at https://www.ecad.eu/download/ensembles/ensembles.php. The UKCP09 climate dataset for the UK is available, following registration, at https://www.metoffice.gov.uk/climatechange/science/monitoring/ukcp09/download/index.html. The ERG5 Eraclito climate dataset for the Emilia-Romagna region is publicly available at https://www.arpae.it/dettaglio_documento.asp?id=6147&idlivello=1528. The climate projections of the NASA NEX-GDDP project are available, following registration, at https://cds.nccs.nasa.gov/nex-gddp/. Population density data from GPWv4 is publicly available, following registration, at http://sedac.ciesin.columbia.edu/data/collection/gpw-v4. Model scripts are available in the electronic supplementary material.

Authors' contributions. S.M. and A.P.M. designed the study and developed the model together with C.C. and M.B. S.M. conducted the analysis and wrote the paper with inputs and comments from all co-authors.

Competing interests. We declare we have no competing interests.

Funding. The research was funded by the National Institute for Health Research Health Protection Research Unit (NIHR HPRU) in Emerging and Zoonotic Infections at the University of Liverpool in partnership with Public Health England (PHE) and Liverpool School of Tropical Medicine (LSTM). The views expressed are those of the authors and not necessarily those of the NHS, the NIHR, the Department of Health or Public Health England.

Acknowledgements. We acknowledge the E-OBS dataset from the EU-FP6 project ENSEMBLES (http://ensembles-eu.metoffice.com) and the data providers in the ECA&D project (http://www.ecad.eu). The UKCP09 data have been made available by the Department for Environment, Food and Rural Affairs (Defra) and Department for Energy and Climate Change (DECC) under licence from the Met Office, Newcastle University, University of East Anglia and Proudman Oceanographic Laboratory. These organizations accept no responsibility for any inaccuracies or omissions in the data, nor for any loss or damage directly or indirectly caused to any person or body by reason of, or arising out of, any use of these data. Future climate scenarios used were taken from the NEX-GDDP dataset, prepared by the Climate Analytics Group and NASA Ames Research Center using the NASA Earth Exchange, and distributed by the NASA Center for Climate Simulation (NCCS).

Reference

1. Hulme PE. 2009 Trade, transport and trouble: managing invasive species pathways in an era of globalization. *J. Appl. Ecol.* **46**, 10–18. (doi:10.1111/jpe.2009.46.issue-1)
2. Williams F *et al.* 2010 The economic cost of invasive non-native species on Great Britain. Cab/001/09, pp. 1–199.
3. Vaux AGC, Medlock JM. 2015 Current status of invasive mosquito surveillance in the UK. *Parasit. Vectors* **8**, 351. (doi:10.1186/s13071-015-0936-9)
4. Lacour G, Chanaud L, L'Ambert G, Hance T. 2015 Seasonal synchronization of diapause phases in *Aedes albopictus* (Diptera: Culicidae). *PLoS ONE* **10**, 1–16. (doi:10.1371/journal.pone.0145311)
5. Adhami J, Reiter P. 1998 Introduction and establishment of *Aedes* (*Stegomyia*) *albopictus* Skuse (Diptera: Culicidae) in Albania. *J. Am. Mosq. Control Assoc.* **14**, 340–343.
6. Sabatini A, Raineri V, Trovato G, Coluzzi M. 1990 *Aedes albopictus* in Italy and possible diffusion of the species into the Mediterranean area. *Parassitologia* **32**, 301–304.
7. Scholte EJ, Dijkstra E, Blok H, De Vries A, Takken W, Hofhuis A, Koopmans M, De Boer A, Reusken CBEM. 2008 Accidental importation of the mosquito *Aedes albopictus* into the Netherlands: a survey of mosquito distribution and the presence of dengue virus. *Med. Vet. Entomol.* **22**, 352–358. (doi:10.1111/mve.2008.22.issue-4)
8. European Centre for Disease Prevention and Control and European Food Safety Authority. 2018 *Aedes albopictus*—current known distribution: January 2018. See https://ecdceuropaeu/en/disease-vectors/surveillance-and-disease-data/mosquito-maps.
9. Grard G, Caron M, Mombo IM, Nkoghe D, Ondo SM, Jiolle D, Fontenille D, Paupy C, Leroy EM. 2014 Zika virus in Gabon (Central Africa)—2007: a new threat from *Aedes albopictus*? *PLoS Neglect. Trop. Dis.* **8**, 1–6. (doi:10.1371/journal.pntd.0002681)
10. Gratz NG. 2004 Critical review of *Aedes albopictus*. *Med. Vet. Entomol.* **18**, 215–227. (doi:10.1111/mve.2004.18.issue-3)
11. Rezza G. *et al.* 2007 Infection with chikungunya virus in Italy: an outbreak in a temperate region. *Lancet* **370**, 1840–1846. (doi:10.1016/S0140-6736(07)61779-6)
12. Schaffner F, Mathis A. 2014 Dengue and dengue vectors in the WHO European region: past, present, and scenarios for the future. *Lancet Infect. Dis.* **14**, 1271–1280. (doi:10.1016/S1473-3099(14)70834-5)
13. Venturi G. *et al.* 2017 Detection of a chikungunya outbreak in central Italy, August to September 2017. *Euro Surveill.* **22**, 17-00646. (doi:10.2807/1560-7917.ES.2017.22.39.17-00646)
14. Niebylski ML, Savage HM, Nasci RS, Craig GB. 1994 Blood hosts of *Aedes albopictus* in the United States. *J. Am. Mosq. Control Assoc.* **10**, 447–450.
15. Kamgang B, Nchoutpouen E, Simard F, Paupy C. 2012 Notes on the blood-feeding behavior of *Aedes albopictus* (Diptera: Culicidae) in Cameroon. *Parasit. Vectors* **5**, 57. (doi:10.1186/1756-3305-5-57)
16. Medlock JM, Vaux AG, Cull B, Schaffner F, Gillingham E, Pfluger V, Leach S. 2017 Detection of the invasive mosquito species *Aedes albopictus* in southern England. *Lancet Infect. Dis.* **17**, 140. (doi:10.1016/S1473-3099(17)30024-5)
17. Public Health England 2017 Mosquito: nationwide surveillance. See https://www.gov.uk/government/publications/mosquito-surveillance/mosquito-nationwide-surveillance.
18. Medlock JM, Avenell D, Barrass I, Leach S. 2006 Analysis of the potential for survival and seasonal activity of *Aedes albopictus* (Diptera: Culicidae) in the United Kingdom. *J. Vector Ecol.: J. Soc. Vector Ecol.* **31**, 292–304. (doi:10.3376/1081-1710(2006)31[292:AOTPFS]2.0.CO;2)
19. Fischer D, Thomas SM, Niemitz F, Reineking B, Beierkuhnlein C. 2011 Projection of climatic suitability for *Aedes albopictus* Skuse (Culicidae) in Europe under climate change conditions. *Glob. Planet. Change* **78**, 54–64. (doi:10.1016/j.gloplacha.2011.05.008)
20. Caminade C, Medlock JM, Ducheyne E, McIntyre KM, Leach S, Baylis M, Morse AP. 2012 Suitability of European climate for the Asian tiger mosquito *Aedes albopictus*: recent trends and future scenarios. *J. R. Soc. Interface* **9**, 2708–2717. (doi:10.1098/rsif.2012.0138)
21. Erickson RA, Presley SM, Allen LJS, Long KR, Cox SB. 2010 A stage-structured, *Aedes albopictus* population model. *Ecol. Modell.* **221**, 1273–1282. (doi:10.1016/j.ecolmodel.2010.01.018)
22. Tran A *et al.* 2013 A rainfall- and temperature-driven abundance model for *Aedes albopictus* populations. *Int. J. Environ. Res. Public Health* **10**, 1698–1719. (doi:10.3390/ijerph10051698)
23. Jia P, Lu L, Chen X, Chen J, Guo L, Yu X, Liu Q. 2016 A climate-driven mechanistic population model of *Aedes albopictus* with diapause. *Parasit. Vectors* **9**, 175. (doi:10.1186/s13071-016-1448-y)
24. Erguler K, Smith-Unna SE, Waldock J, Proestos Y, Christophides GK, Lelieveld J, Parham PE. 2016

Large-scale modelling of the environmentally-driven population dynamics of temperate *Aedes albopictus* (Skuse). *PLoS ONE* **11**, 1–28. (doi:10.1371/journal.pone.0149282)

25. Mohammed A, Chadee DD. 2011 Effects of different temperature regimens on the development of *Aedes aegypti* (L.) (Diptera: Culicidae) mosquitoes. *Acta Trop.* **119**, 38–43. (doi:10.1016/j.actatropica.2011.04.004)
26. Richardson K, Hoffmann AA, Johnson P, Ritchie S, Kearney MR. 2011 Thermal sensitivity of *Aedes aegypti* from Australia: empirical data and prediction of effects on distribution. *J. Med. Entomol.* **48**, 914–923. (doi:10.1603/ME10204)
27. Carrington LB, Seifert SN, Willits NH, Lambrechts L, Scott TW. 2013 Large diurnal temperature fluctuations negatively influence *Aedes aegypti* (Diptera: Culicidae) life-history traits. *J. Med. Entomol.* **50**, 43–51. (doi:10.1603/ME11242)
28. Ma G, Hoffmann AA, Ma CS. 2015 Daily temperature extremes play an important role in predicting thermal effects. *J. Exp. Biol.* **218**, 2289–2296. (doi:10.1242/jeb.122127)
29. Chen S, Fleischer SJ, Saunders MC, Thomas MB. 2015 The influence of diurnal temperature variation on degree-day accumulation and insect life history. *PLoS ONE* **10**, e0120772. (doi:10.1371/journal.pone.0120772)
30. Vasseur DA, DeLong JP, Gilbert B, Greig HS, Harley CD, McCann KS, Savage V, Tunney TD, O'Connor MI. 2014 Increased temperature variation poses a greater risk to species than climate warming increased temperature variation poses a greater risk to species than climate warming. *Proc. R. Soc. B* **281**, 20132612. (doi:10.1098/rspb.2013.2612)
31. Beck-Johnson L, Nelson W, Paaijmans K, Read A, Thomas M, Bjørnstad O. 2017 The importance of temperature fluctuations in understanding mosquito population dynamics and malaria risk. *R. Soc. open sci.* **4**, 160969. (doi:10.1098/rsos.160969)
32. Delatte H, Gimonneau G, Triboire A, Fontenille D. 2009 Influence of temperature on immature development, survival, longevity, fecundity, and gonotrophic cycles of *Aedes albopictus*, vector of chikungunya and dengue in the Indian ocean. *J. Med. Entomol.* **46**, 33–41. (doi:10.1603/033.046.0105)
33. Paupy C, Delatte H, Bagny L, Corbel V, Fontenille D. 2009 *Aedes albopictus*, an arbovirus vector: from the darkness to the light. *Microbes Infect.* **11**, 1177–1185. (doi:10.1016/j.micinf.2009.05.005)
34. Toma L, Severini F, Di Luca M, Bella A, Romi R. 2003 Seasonal patterns of oviposition and egg hatching rate of *Aedes albopictus* in Rome. *J. Am. Mosq. Control Assoc.* **19**, 19–22.
35. Cailly P, Tran A, Balenghien T, L'Ambert G, Toty C, Ezanno P. 2012 A climate-driven abundance model to assess mosquito control strategies. *Ecol. Modell.* **227**, 7–17. (doi:10.1016/j.ecolmodel.2011.10.027)
36. Briegel H, Timmermann SE. 2001 *Aedes albopictus* (Diptera: Culicidae): physiological aspects of development and reproduction. *J. Med. Entomol.* **38**, 566–571. (doi:10.1603/0022-2585-38.4.566)
37. White MT, Griffin JT, Churcher TS, Ferguson NM, Basáñez Mg Ghani AC. 2011 Modelling the impact of vector control interventions on *Anopheles gambiae* population dynamics. *Parasit. Vectors* **4**, 153. (doi:10.1186/1756-3305-4-153)
38. Abdelrazec A, Gumel AB. 2017 Mathematical assessment of the role of temperature and rainfall on mosquito population dynamics. *J. Math. Biol.* **74**, 1351–1395. (doi:10.1007/s00285-016-1054-9)
39. Marini F, Caputo B, Pombi M, Tarsitani G, Della-Torre A. 2010 Study of *Aedes albopictus* dispersal in Rome, Italy, using sticky traps in mark–release–recapture experiments. *Med. Vet. Entomol.* **24**, 361–368. (doi:10.1111/j.1365-2915.2010.00898.x)
40. de-Wit CT. 1978 *Simulation of assimilation, respiration and transpiration of crops*. Wageningen, the Netherlands: Pudoc.
41. Reicosky DC, Winkelman LJ, Baker JM, Baker DG. 1989 Accuracy of hourly air temperatures calculated from daily minima and maxima. *Agric. For. Meteorol.* **46**, 193–209. (doi:10.1016/0168-1923(89)90064-6)
42. Forsythe WC, Rykiel EJ, Stahl RS, Wu Hi, Schoolfield RM. 1995 A model comparison for daylength as a function of latitude and day of year. *Ecol. Modell* **80**, 87–95. (doi:10.1016/0304-3800(94)00034-F)
43. Haylock MR, Hofstra N, Klein-Tank AMG, Klok EJ, Jones PD, New M. 2008 A European daily high-resolution gridded data set of surface temperature and precipitation for 1950–2006. *J. Geophys. Res. Atmos.* **113**, D20119. (doi:10.1029/2008JD010201)
44. Jenkins GJ, Perry MC, Prior MJ. 2009 The climate of the UK and recent trends.
45. Antolini G, Auteri L, Pavan V, Tomei F, Tomozeiu R, Marletto V. 2016 A daily high-resolution gridded climatic data set for Emilia-Romagna, Italy, during 1961–2010. *Int. J. Climatol.* **36**, 1970–1986. (doi:10.1002/joc.2016.36.issue-4)
46. Thrasher B, Maurer EP, McKellar C, Duffy PB. 2012 Technical note: bias correcting climate model simulated daily temperature extremes with quantile mapping. *Hydrol. Earth Syst. Sci.* **16**, 3309–3314. (doi:10.5194/hess-16-3309-2012)
47. Doxsey-Whitfield E, MacManus K, Adamo SB, Pistolesi L, Squires J, Borkovska O, Baptista S. 2015 Taking advantage of the improved availability of census data: a first look at the gridded population of the world, version 4. *Pap. Appl. Geogr.* **1**, 226–234. (doi:10.1080/23754931.2015.1014272)
48. Office For National Statistics 2017 National population projections: 2016-based projections, methodology. See https://www.ons.gov.uk/peoplepopulationandcommunity/populationandmigration/populationprojections.
49. Kraemer MUG *et al.*2015 The global distribution of the arbovirus vectors *Aedes aegypti* and *Ae. albopictus*. *eLife* **4**, 1–18. (doi:10.7554/eLife.08347)
50. Akiner MM, Demirci B, Babuadze G, Robert V, Schaffner F. 2016 Spread of the invasive mosquitoes *Aedes aegypti* and *Aedes albopictus* in the black sea region increases risk of chikungunya, dengue, and Zika outbreaks in europe. *PLoS Neglect. Trop. Dis.* **10**, 1–5. (doi:10.1371/journal.pntd.0004664)
51. Walther D, Scheuch DE, Kampen H. 2017 The invasive Asian tiger mosquito *Aedes albopictus* (Diptera: Culicidae) in Germany: local reproduction and overwintering. *Acta Trop.* **166**, 186–192. (doi:10.1016/j.actatropica.2016.11.024)
52. Di Luca M *et al.* 2017 First record of the invasive mosquito species *Aedes* (*Stegomyia*) *albopictus* (Diptera: Culicidae) on the southernmost Mediterranean islands of Italy and Europe. *Parasit. Vectors* **10**, 543. (doi:10.1186/s13071-017-2488-7)
53. Osório H, Zé-Zé L, Neto M, Silva S, Marques F, Silva A, Alves M. 2018 Detection of the invasive mosquito species *Aedes* (*Stegomyia*) *albopictus* (Diptera: Culicidae) in Portugal. *Int. J. Environ. Res. Public Health* **15**, 820. (doi:10.3390/ijerph15040820)
54. Meineke EK, Dunn RR, Sexton JO, Frank SD. 2013 Urban warming drives insect pest abundance on street trees. *PLoS ONE* **8**, 2–8. (doi:10.1371/journal.pone.0059687)
55. Morris MD. 1991 Factorial plans for preliminary sampling computational experiments. *Technometrics* **33**, 161–174. (doi:10.1080/00401706.1991.10484804)
56. McKay MD, Beckman RJ, Conover WJ. 2000 A comparison of three methods for selecting values of input variables in the analysis of output from a computer code. *Technometrics* **42**, 55–61. (doi:10.1080/00401706.2000.10485979)
57. Pianosi F, Sarrazin F, Wagener T. 2015 A Matlab toolbox for global sensitivity analysis. *Environ. Model. Softw.* **70**, 80–85. (doi:10.1016/j.envsoft.2015.04.009)
58. Thomas S, Obermayr U, Fischer D, Kreyling J, Beierkuhnlein C. 2012 Low-temperature threshold for egg survival of a post-diapause and non-diapause European aedine strain, *Aedes albopictus* (Diptera: Culicidae). *Parasit. Vectors* **5**, 100. (doi:10.1186/1756-3305-5-100)
59. Urbanski J, Mogi M, O'Donnell D, DeCotiis M, Toma T, Armbruster P. 2012 Rapid adaptive evolution of photoperiodic response during invasion and range expansion across a climatic gradient. *Am. Nat.* **179**, 490–500. (doi:10.1086/664709)
60. Brady J *et al.* 2013 Modelling adult *Aedes aegypti* and *Aedes albopictus* survival at different temperatures in laboratory and field settings. *Parasit. Vectors* **6**, 351. (doi:10.1186/1756-3305-6-351)
61. Lacour G, Vernichon F, Cadilhac N, Boyer S, Lagneau C, Hance T. 2014 When mothers anticipate: effects of the prediapause stage on embryo development time and of maternal photoperiod on eggs of a temperate and a tropical strains of *Aedes albopictus* (Diptera: Culicidae). *J. Insect. Physiol.* **71**, 87–96. (doi:10.1016/j.jinsphys.2014.10.008)
62. Rozilawati H, Masri SM, Tanaselvi K, Zairi J, Nazn W, Lee H. 2016 Effect of temperature on the immature development of *Aedes albopictus* Skuse. *Southeast Asian J. Trop. Med. Public Health* **47**, 731–746. (doi:10.1111/j.1365-2915.2011.00971.x)

63. Kreß A, Oppold AM, Kuch U, Oehlmann J, Müller R. 2017 Cold tolerance of the Asian tiger mosquito *Aedes albopictus* and its response to epigenetic alterations. *J. Insect. Physiol.* **99**, 113–121. (doi:10.1016/j.jinsphys.2017.04.003)
64. Paaijmans KP, Blanford S, Bell AS, Blanford JI, Read AF, Thomas MB. 2010 Influence of climate on malaria transmission depends on daily temperature variation. *Proc. Natl Acad. Sci. USA* **107**, 15 135–15 139. (doi:10.1073/pnas.1006422107)
65. Lambrechts L, Paaijmans KP, Fansiri T, Carrington LB, Kramer LD, Thomas MB, Scott TW. 2011 Impact of daily temperature fluctuations on dengue virus transmission by *Aedes aegypti*. *Proc. Natl Acad. Sci. USA* **108**, 7406–7465. (doi:10.1073/pnas.1101377108)
66. Wang X, Tang S, Cheke RA. 2016 A stage structured mosquito model incorporating effects of precipitation and daily temperature fluctuations. *J. Theor. Biol.* **411**, 27–36. (doi:10.1016/j.jtbi.2016.09.015)
67. ECDC. 2012 The climatic suitability for dengue transmission in continental Europe. Technical report. See https://ecdc.europa.eu/sites/portal/files/media/en/publications/Publications/TER-Climatic-suitablility-dengue.pdf.
68. Dieng H, Saifur RGM, Hassan AA, Che Salmah MR, Boots M, Satho T, Jaal Z, AbuBaskar S. 2010 Indoor-breeding of *Aedes albopictus* in northern peninsular Malaysia and its potential epidemiological implications. *PLoS ONE* **5**, e11790. (doi:10.1371/journal.pone.0011790)
69. Benedict MQ, Levine RS, Hawley WA, Lounibos LP. 2007 Spread of the tiger: global risk of invasion by the mosquito *Aedes albopictus*. *Vector Borne Zoonotic Dis.* **7**, 76–85. (doi:10.1089/vbz.2006.0562)
70. Liu-Helmersson J, Quam M, Wilder-Smith A, Stenlund H, Ebi K, Massad E, Rocklöv J. 2016 Climate change and Aedes vectors: 21st century projections for dengue transmission in europe. *EBioMedicine* **7**, 267–277. (doi:10.1016/j.ebiom.2016.03.046)
71. Gould EA, Higgs S, Buckley A, Gritsun TS. 2006 Potential arbovirus emergence and implications for the United Kingdom. *Emerg. Infect. Dis.* **12**, 549–555. (doi:10.3201/eid1204.051010)
72. Genchi C, Bowman D, Drake J. 2014 Canine heartworm disease (*Dirofilaria immitis*) in Western Europe: survey of veterinary awareness and perceptions. *Parasit. Vectors* **7**, 1–7. (doi:10.1186/1756-3305-7-206)
73. Aranda C, Eritja R, Roiz D. 2006 First record and establishment of the mosquito *Aedes albopictus* in Spain. *Med. Vet. Entomol.* **20**, 150–152. (doi:10.1111/mve.2006.20.issue-1)
74. Roche B, Léger L, L'Ambert G, Lacour G, Foussadier R, Besnard G, Barré-Cardi H, Simard F, Fontenille D. 2015 The spread of *Aedes albopictus* in metropolitan France: contribution of environmental drivers and human activities and predictions for a near future. *PLoS ONE* **10**, e0125600. (doi:10.1371/journal.pone.0125600)
75. Public Health England. 2018 Qualitative assessment of the risk that chikungunya virus presents to the UK population. See https://assets.publishing.service.gov.uk/government/uploads/system/uploads/attachment_data/file/702070/Chikungunya_risk_assessment.pdf.